Pharmacological Inhibition of eIF2α Phosphorylation by ISRIB Ameliorates Vascular Calcification in rats

Jianlong Dong[a#], Sheng Jin[a, b, c#], Jingjing Guo[a], Rui Yang[a], Danyang Tian[a], Hongmei Xue[a], Lin Xiao[a], Qi Guo[a], Ru Wang[a], Meng Xu[a], Xu Teng[a, b, c], Yuming Wu[a, b, c]

[a] Department of Physiology, Hebei Medical University, Shijiazhuang, China, 050017

[b] Hebei Collaborative Innovation Center for Cardio–cerebrovascular Disease, Shijiazhuang, China, 050017

[c] Hebei Key Laboratory of Neurophysiology, Shijiazhuang, China, 050017

# The first two authors contributed equally.

Short Title: ISRIB ameliorates VC

Corresponding author:

Xu Teng, Zhongshan East Road No.361, Shijiazhuang, China, 050017

Tel: +86-311-86266464

email: tengxu78@163.com

Yuming Wu, Zhongshan East Road No.361, Shijiazhuang, China, 050017

Tel: +86-311-86261288

email: wuyum@yahoo.com

Summary

Vascular calcification (VC) is an independent risk factor for cardiovascular events and all-cause mortality with the absence of current treatment. This study aimed to investigate whether eIF2α phosphorylation inhibition could ameliorate VC. VC in rats was induced by administration of vitamin D_3 (3×10^5 IU / kg, intramuscularly) plus nicotine (25 mg / kg, intragastrically). ISRIB (0.25 mg/kg·week), an inhibitor of eIF2α phosphorylation, ameliorated the elevation of calcium deposition and ALP activity in calcified rat aortas, accompanied by amelioration of increased SBP, PP, and PWV. The decreased protein levels of calponin and SM22α, and the increased levels of RUNX2 and BMP2 in calcified aorta were all rescued by ISRIB, while the increased levels of the GRP78, GRP94, and C/EBP homologous proteins in rats with VC were also attenuated. Moreover, ISRIB could prevent the elevation of eIF2α phosphorylation and ATF4, and partially inhibit PERK phosphorylation in the calcified aorta. These results suggested that an eIF2α phosphorylation inhibitor could ameliorate VC pathogenesis by blocking eIF2α/ATF4 signaling, which may provide a new target for VC prevention and treatment.

Keywords: vascular calcification; endoplasmic reticulum stress; eIF2; aorta; ISRIB

Introduction

Vascular calcification (VC) is the ectopic deposition of inorganic calcium phosphate crystals in the blood vessel walls [1], which results in a three- to fourfold higher cardiovascular and all-cause mortality [2]. VC is usually divided into intimal (exclusively linked with atherosclerosis) and medial (widely linked with hypertension, chronic kidney disease, and diabetes) calcifications according to its location in the blood vessel wall [3]. The production of medial VC directly results in blood-vessel-wall stiffening and arterial-compliance impairment, which can cause various cardiovascular complications including systolic hypertension and aortic stenosis. A bidirectional causal association between hypertension and arterial stiffness [4] in turn gives rise to cardiac hypertrophy [5] and reduces the blood supply to the heart and peripheral organs, all of which can eventually result in congestive heart failure and even death [6]. However, no early detection methods and no proven effective treatment to prevent or reverse VC currently exist [7].

The endoplasmic reticulum (ER) is the largest organelle in eukaryotic cells and it has various functions, including protein folding, modification, and transportation; calcium restoration; and lipids synthesis. The perturbation of its homeostasis, i.e., ER stress (ERS), increases the accumulation of unfolded or misfolded proteins inside the ER lumen, which stimulates three sensors located in the ER membrane (i.e., the protein kinase RNA-like endoplasmic reticulum kinase [PERK], IRE1, and the activating transcription factor 4 [ATF4]), and

triggers the unfolded protein response, which is associated signaling cascades. Prolonged ERS response leads to further cellular injury and even death (apoptosis or autophagy), although ERS activation primarily aims to restore ER homeostasis [8, 9]. This paper firstly demonstrated ERS-associated apoptosis of vascular smooth muscle cells (VSMCs) in the calcified aorta in rats [10] and further confirmed the contribution of ATF4-mediated apoptosis to VC progression [11]. The exaggerated role of ERS in VC has also been supported by many other studies [12-18], and inhibition of ERS might be used for VC prevention and therapy [19-21].

The role of the PERK/eukaryotic initiation factor 2 alpha (eIF2α)/ATF4/C/EBP homologous protein (CHOP) signaling in VC progression is the most widely investigated among the three branches [11-14, 17]. The knockdown of PERK, ATF4, or CHOP was shown to significantly ameliorate the calcification of VSMCs in vitro. However, the effect of eIF2α inhibition on VC as well as whether inhibition of the PERK cascade could ameliorate VC in vivo remain unknown. Given that treatment by drugs is far more practical than by genetic techniques in clinical practice, the current study determined the ameliorative effect of the inhibition of eIF2α phosphorylation by ISRIB on VC progression in rats treated with nicotine plus vitamin D3 (VDN).

Methods

The data that support the findings of this study are available from the

corresponding author upon reasonable request.

Experimental procedure

All animal care and experimental protocols followed the PR China Animal Management Rule (documentation number 55, 2001, the Ministry of Health of PR China) and the Guide for the Care and Use of Laboratory Animals (1985), NIH, Bethesda, and were approved by the Animal Care Committee of Hebei Medical University. Male Sprague–Dawley (SD) rats (200–220 g) were supplied by the Animal Center of Hebei Medical University. All animals were housed at 22 ± 2 °C with a relative humidity of 50% ± 10% and a 12:12-h light/dark cycle. The animals had free access to water and standard chow pellets.

Thirty-two rats were randomly divided into the following four groups (n = 8 in each group): (1) the control group (Con), treated with the vehicles; (2) the ISRIB group, intraperitoneally injected with 0.25 mg/kg·week ISRIB (SML0843; Sigma-Aldrich LLC, Saint Louis, MO, USA) for 4 weeks; (3) the VC model produced by VDN; and (4) the VC plus ISRIB treatment group (VC + IRSIB). The ISRIB was solved originally with DMSO at 1 mg/ml, and diluted with normal saline at final concentration of 0.05 mg/ml. The rats were anesthetized with sodium pentobarbital (50 mg/kg) for further determination after 4 weeks of treatment.

VC model production in rats

The rat VC model was created as previously described [22, 23]. SD rats

were intramuscularly injected with 300,000 IU/kg vitamin D_3 (47763; Sigma-Aldrich LLC) dissolved in 0.5 mL medical oil for injection and intragastrically treated with 25 mg/kg nicotine (755729; Sigma-Aldrich LLC) in 5 mL peanut oil at 9:00 am on day 1. Nicotine was readministered at 9:00 pm on the same day. Vitamin D3 was reinjected at 9:00 am on days 2 and 15. The rats in the control group were administered the corresponding solvents. The rats were raised 4 weeks after the first injection of nicotine, and then anesthetized with sodium pentobarbital (50 mg/kg) for measuring hemodynamic parameters.

Measurement of arterial blood pressure and pulse wave velocity

Arterial blood pressure (BP) and pulse wave velocity (PWV) were determined by arterial catheter as previously reported with minor modifications [24, 25]. The rats were anesthetized with an intraperitoneal urethane injection (1 g/kg) 4 weeks after the beginning of treatment. For BP and PWV measurements, a catheter (BB31695-PE/3; Scientific Commodities Inc., Lake Havasu, AZ, USA) connected to a pressure transducer was located at the left common carotid artery, and another catheter was located at the right femoral artery, respectively. The blood pressure waves from the two transducers were simultaneously imported to a recorder system (Chengdu Techman Software Co., Ltd., Chengdu, China). Systolic blood pressure (SBP) and pulse pressure (PP) were calculated when arterial pressure had been stable for 15 min. The transit time for the pulse wave moving from the aorta to the femoral artery was

obtained from the foot-to-foot delay between the simultaneously recorded pressure waves. PWV was calculated from the transit time and distance between the two recording sites. After determination of the hemodynamic parameters, the rats were euthanized and then the aorta were collected.

VC evaluation in the aorta

One segment of thoracic aortas about 0.5 cm were fixed in 4% paraformaldehyde for 12 h, embedded in paraffin, cut into 6-μm-thick sections, and stained with 2% pH 4.1 Alizarin red S (A5533; Sigma-Aldrich LLC) to measure calcium deposition in the vessel wall.

Another segment of the thoracic aortas about 1 cm without adventitia was dried at 55 °C in heating blocks and weighed. The tissues were then dissolved in 0.6 N HCl, and the supernatant fluid was used to measure calcium content using a commercial kit (C004-2-1; Jiancheng Bioengineering Institute, Nanjing, China) as per manufacturer's instructions. The data were normalized to the aortic dry weight.

Another segment of the thoracic aortas about 1 cm was homogenized with saline, and the alkaline phosphatase (ALP) activity in lysis was determined using a commercial kit (A059-2-2; Jiancheng Bioengineering Institute) according to the manufacturer's instructions. Another 50 μL lysis was valued protein contents with a bicinchoninic acid commercial kit (P1513; Applygen Technologies Inc., Beijing, China). Results were normalized to the total protein

level.

Western blot

Aortas were collected and homogenized in RIPA lysis buffer (C1055; Applygen Technologies Inc.). The lysate protein concentrations were determined using a bicinchoninic acid commercial kit as previously. A proportional volume of 5 × loading buffer (B1012; Applygen Technologies Inc.) was added, and the samples were boiled for 10 min. Samples of equal-weight protein underwent 10% SDS-polyacrylamide gel electrophoresis for 3 h at 60 mA. The proteins were then electrophoretically transferred onto a nitrocellulose membrane (sc-3724; Santa Cruz Biotechnology Inc., Dallas, TX, USA), which was incubated for 1 h in tris-buffered saline containing 1% bovine serum albumin (SRE0096; Sigma-Aldrich LCC). The membranes were incubated with primary antibody at 4 °C overnight, washed three times for 10 min each in tris-buffered saline–Tween 20 (TBST), and incubated in secondary antibody for 1 h. The membranes were then washed three times for 10 min each in TBST and enhanced chemiluminescence detection (P1050; Applygen Technologies Inc.) was performed. Autoradiographs were scanned, and the relative densities were quantified by ImageJ 1.48v. Sources and dilutions of the antibodies are shown in Table 1.

Statistical analysis

The data were presented as means ± SD and analyzed by GraphPad Prism 8.2.1 (GraphPad Software Inc., San Diego, CA, USA). The data, detected by Shapiro–Wilk test, were all normally distributed. One-way analysis of variance followed by a post hoc Tukey test was used for multiple comparisons. A *P* value of <0.05 was considered significant.

Results

Ameliorative effect of ISRIB on VC in rats with VDN

Alizarin red staining, calcium content, and ALP activity in the aorta were used to determine whether ISRIB could ameliorate VC progression. Alizarin red staining showed calcium deposition in the tunica media of rats with VDN, which were significantly ameliorated by ISRIB (Fig. 1A). The aortic structure was normal and well-organized in the control and ISRIB-alone groups (Fig. 1A). The calcium content and ALP activity of aortic tissue were both consistently significantly increased in the VC group compared with the control group (Figs. 1B and 1C). The increased calcium content and ALP activity in the calcified aorta were rescued by ISRIB treatment (Figs. 1B and 1C). Moreover, ISRIB-alone treatment did not affect these two indicators (Fig. 1B and 1C).

Ameliorative effect of ISRIB on aortic stiffness induced by VC

VC can lead to aortic stiffness, resulting in impairment of cardiac function

and blood supply to peripheral organs. SBP, PP, and PWV were measured in this study to determine aortic stiffness. Rats treated with VDN showed increased SBP, PP, and PWV compared with the control group (Fig. 2). ISRIB treatment significantly rescued the increased levels of SBP, PP, and PWV in rats with VC (Fig. 2). Moreover, ISRIB alone did not affect these three indicators compared with the control group (Fig. 2).

Ameliorative effect of ISRIB on osteoblastic differentiation of VSMCs in calcified aorta

Two markers of contractile VSMCs (i.e., calponin and SM22α) and two markers of osteoblast-differentiated VSMCs (i.e., RUNX2 and BMP2) were detected by Western blot to determine the transdifferentiation of VSMCs for contractile to osteoblastic phenotype. The protein levels of calponin and SM22α in the aorta of VC rats were significantly decreased compared with those in the control group (Fig. 3); this was rescued by ISRIB treatment (Fig. 3). Conversely, the protein levels of RUNX2 and BMP2 in the aorta of VC rats were higher compared with those in the control rats (Fig. 3), and ISRIB treatment significantly attenuated these increased protein levels in the calcified aorta (Fig. 3). No effect on the protein levels of RUNX2 and BMP2 by ISRIB alone was noted compared with the control group (Fig. 3).

Ameliorative effect of ISRIB on ERS activation in the calcified aorta

Three markers of ERS (i.e., GRP78, GRP94, and CHOP) were detected by Western blot to determine the ERS activation in the aortic tissue. The protein levels of GRP78, GRP94, and CHOP in the aorta of rats with VC were significantly increased compared with those in the control group (Fig. 4). The increased protein levels in the calcified aorta were rescued by ISRIB treatment (Fig. 4). No effect of ISRIB alone was noted on the levels of these proteins compared with the control group (Fig. 4).

Ameliorative effect of ISRIB on eIF2/ATF4 activation in the calcified aorta

Protein levels of phosphorylated PERK, phosphorylated eIF2, and ATF4 were detected by Western blot to determine the activation of the eIF2/ATF4 signaling pathway in the aortic tissue. The phosphorylated PERK, phosphorylated eIF2, and ATF4 protein levels in the aorta of rats with VC were significantly increased compared with those in the control group (Fig. 5). The increased protein levels of phosphorylated eIF2 and ATF4 in the calcified aorta were rescued by ISRIB treatment, while those of phosphorylated PERK were partially restored (Fig. 5). No effect of ISRIB alone on the levels of these proteins was noted compared with the control group (Fig. 5).

Discussion

This study showed that ISRIB, an inhibitor of eIF2 phosphorylation, significantly ameliorates calcium deposition and increases ALP activity in the calcified aorta of rats, accompanied by the amelioration of increased SBP, PP, and PWV. The decreased protein levels of calponin–SM22α and RUNX2–BMP2 in the calcified aorta were all rescued by ISRIB treatment, while the increased levels of GRP78, GRP94, and CHOP in rats with VC were also attenuated. ISRIB could almost totally prevent the elevation of eIF2 and ATF4 phosphorylation in the calcified aorta and partially inhibit PERK phosphorylation.

The VC model in rats induced by vitamin D3 plus nicotine was first reported in 1997 [22] and extensively used in animal investigation [26]. A previous study successfully established the VC model by vitamin D3 plus nicotine in rats [20, 21]. The current study also observed the calcium deposition in tunica media by Alizarin red staining and the increased levels of calcium contents and ALP activity in the aorta of rats with vitamin D3 plus nicotine. These results supported the establishment of aortic calcification in rats.

The aortic distensibility and stiffness are crucial in blood circulation because it provides vascular buffering to each of the left ventricular contractions aside from the function of simple tunnels for blood flows. Aortic stiffness represents the loss of compliance in aortic walls that contributed to hypertension and its related organ damage, including the heart, brain, and kidneys, and then increased all-cause mortality independent of standard

cardiovascular risk factors [27, 28]. Aortic stiffness can cause a series of hemodynamic sequelae, including increased SBP, PP, and PWV [29]. Increased PWV has particularly been widely recognized as a reliable and accurate method to quantify aortic stiffness [30]. VC is one of the important mechanisms leading to stiffness and impaired aortic compliance [31, 32]. Several clinical studies have suggested that VC may be causally linked to arterial stiffness in subjects of different ages [33, 34]. Increased SBP, PP, and PWV in the current study supported the aortic stiffness in rats with VC, which could be significantly ameliorated by ISRIB.

A series of articles have demonstrated that ERS plays a critical role in VC pathogenesis [10, 16]. Among the three signaling branches activated by ERS, PERK/eIF2/ATF4 has been substantially shown to contribute to VC progression via the induction of osteoblastic differentiation in VSMCs [12, 13, 17]. The current study observed that ISRIB, blocking PERK/eIF2/ATF4 signaling cascade via the inhibition of eIF2 phosphorylation, ameliorated the deposition of calcium in the aortic media and the increased calcium content and ALP activity in rats with VC accompanied by the restoration of the protein levels of SM22α, calponin, RUNX2, and BMP2. These results demonstrated that ISRIB can significantly ameliorate osteoblastic differentiation of VSMCs and VC pathogenesis by inhibiting eIF2 phosphorylation.

The results of the current study demonstrated that ISRIB, an inhibitor of eIF2 phosphorylation, can ameliorate VC pathogenesis via blocking

PERK/eIF2/ATF4 signaling. It is believed that this is the first report on the ameliorative effect of inhibiting eIF2 phosphorylation on VC and may provide a new target for VC prevention and treatment.

Acknowledgements

This work is supported by the National Natural Science Foundation of China (31871154, 81770499, 91849120, 31671185), the Association Fund for Precision Medicine of Hebei [CN] (C2020206025), and the Natural Science Foundation of Hebei [CN] (H2020206350).

Conflict of interests Statement

The authors declare that they have no conflict of interests.

References

1. Sage AP, Tintut Y, Demer LL. Regulatory mechanisms in vascular calcification. Nat Rev Cardiol 2010;7:528-536.
2. Rennenberg RJ, Kessels AG, Schurgers LJ, van Engelshoven JM, de Leeuw PW, Kroon AA. Vascular calcifications as a marker of increased cardiovascular risk: a meta-analysis. Vasc Health Risk Manag 2009;5:185-197.
3. Lanzer P, Boehm M, Sorribas V, Thiriet M, Janzen J, Zeller T, St Hilaire C, Shanahan C. Medial vascular calcification revisited: review and perspectives. Eur Heart J 2014;35:1515-1525.
4. Cecelja M, Keehn L, Ye L, Spector TD, Hughes AD, Chowienczyk P. Genetic aetiology of blood pressure relates to aortic stiffness with bi-directional causality: evidence from heritability, blood pressure polymorphisms, and Mendelian randomization. Eur Heart J 2020;41:3314-3322.
5. Ishiyama Y, Hoshide S, Kanegae H, Kario K. Increased Arterial Stiffness Amplifies the Association Between Home Blood Pressure Variability and Cardiac Overload: The J-HOP Study. Hypertension. 2020;75:1600-1606.
6. London GM. Arterial calcification: cardiovascular function and clinical outcome. Nefrologia 2011;31:644-647.
7. Furmanik M, Chatrou M, van Gorp RH, Akbulut A, Willems B, Schmidt HH, van Eys G, Bochaton-Piallat ML, Proudfoot D, Biessen EA, Hedin U,

Matic L, Mees B, Shanahan CM, Reutelingsperger C, Schurgers LJ. Reactive Oxygen-Forming Nox5 Links Vascular Smooth Muscle Cell Phenotypic Switching and Extracellular Vesicle-Mediated Vascular Calcification. Circ Res 2020;127:911-27.

8. Higuchi-Sanabria R, Frankino PA, Paul JW 3rd, Tronnes SU, Dillin A. A Futile Battle? Protein Quality Control and the Stress of Aging. Dev Cell 2018;44:139-163.
9. Bhattarai KR, Chaudhary M, Kim HR, Chae HJ. Endoplasmic Reticulum (ER) Stress Response Failure in Diseases. Trends Cell Biol 2020;30:672-675.
10. Duan X, Zhou Y, Teng X, Tang C, Qi Y. Endoplasmic reticulum stress-mediated apoptosis is activated in vascular calcification. Biochem Biophys Res Commun 2009;387: 694-649.
11. Duan XH, Chang JR, Zhang J, Zhang BH, Li YL, Teng X, Zhu Y, Du J, Tang CS, Qi YF. Activating transcription factor 4 is involved in endoplasmic reticulum stress-mediated apoptosis contributing to vascular calcification. Apoptosis 2013;18:1132-1144.
12. Masuda M, Ting TC, Levi M, Saunders SJ, Miyazaki-Anzai S, Miyazaki M. Activating transcription factor 4 regulates stearate-induced vascular calcification. J Lipid Res 2012;53:1543-1552.

13. Masuda M, Miyazaki-Anzai S, Levi M, Ting TC, Miyazaki M. PERK-eIF2α-ATF4-CHOP signaling contributes to TNFα-induced vascular calcification. J Am Heart Assoc 2013;2:e000238.
14. Miyazaki-Anzai S, Masuda M, Demos-Davies KM, Keenan AL, Saunders SJ, Masuda R, Jablonski K, Cavasin MA, Kendrick J, Chonchol M, McKinsey TA, Levi M, Miyazaki M. Endoplasmic reticulum stress effector CCAAT/enhancer-binding protein homologous protein (CHOP) regulates chronic kidney disease-induced vascular calcification. J Am Heart Assoc 2014;3:e000949.
15. Zhu Q, Guo R, Liu C, Fu D, Liu F, Hu J, Jiang H. Endoplasmic Reticulum Stress-Mediated Apoptosis Contributing to High Glucose-Induced Vascular Smooth Muscle Cell Calcification. J Vasc Res 2015;52:291-298.
16. Panda DK, Bai X, Sabbagh Y, Zhang Y, Zaun HC, Karellis A, Koromilas AE, Lipman ML, Karaplis AC. Defective interplay between mTORC1 activity and endoplasmic reticulum stress-unfolded protein response in uremic vascular calcification. Am J Physiol Renal Physiol 2018;314:F1046-F1061.
17. Furmanik M, Shanahan CM. ER stress regulates alkaline phosphatase gene expression in vascular smooth muscle cells via an ATF4-dependent mechanism. BMC Res Notes 2018;11:483.
18. Dong Q, Chen Y, Liu W, Liu X, Chen A, Yang X, Li Y, Wang S, Fu M, Ou JS, Lu L, Yan J. 25-Hydroxycholesterol promotes vascular calcification via

activation of endoplasmic reticulum stress. Eur J Pharmacol 2020;880:173165.

19. Chang JR, Duan XH, Zhang BH, Teng X, Zhou YB, Liu Y, Yu YR, Zhu Y, Tang CS, Qi YF. Intermedin1-53 attenuates vascular smooth muscle cell calcification by inhibiting endoplasmic reticulum stress via cyclic adenosine monophosphate/protein kinase A pathway. Exp Biol Med (Maywood) 2013;238:1136-1146.
20. Yang R, Teng X, Li H, Xue HM, Guo Q, Xiao L, Wu YM. Hydrogen Sulfide Improves Vascular Calcification in Rats by Inhibiting Endoplasmic Reticulum Stress. Oxid Med Cell Longev 2016;2016:9095242.
21. Hao W, Yang R, Yang Y, Jin S, Li Y, Yuan F, Guo Q, Xiao L, Wang X, Wang F, Wu Y, Teng X. Stellate ganglion block ameliorates vascular calcification by inhibiting endoplasmic reticulum stress. Life Sci. 2018;193:1-8.
22. Niederhoffer N, Bobryshev YV, Lartaud-Idjouadiene I, Giummelly P, Atkinson J. Aortic calcification produced by vitamin D3 plus nicotine. J Vasc Res 1997;34:386-398.
23. Li H, Teng X, Yang R, Guo Q, Xue H, Xiao L, Duan X, Tian D, Feng X, Wu Y. Hydrogen Sulfide Facilitates the Impaired Sensitivity of Carotid Sinus Baroreflex in Rats with Vascular Calcification. Front Pharmacol 2017;8:629.

24. Fitch RM, Vergona R, Sullivan ME, Wang YX. Nitric oxide synthase inhibition increases aortic stiffness measured by pulse wave velocity in rats. Cardiovasc Res 2001;51:351-358.
25. Kameyama H, Takeda K, Kusaba T, Narumiya H, Tanda S, Kuwahara N, Yamada K, Tamagaki K, Okigaki M, Hatta T, Sasaki S. Augmentation of pulse wave velocity precedes vascular structural changes of the aorta in rats treated with N(omega)-nitro-L-arginine methyl ester. Hypertens Res 2005;28:439-445.
26. Herrmann J, Babic M, Tölle M, van der Giet M, Schuchardt M. Research Models for Studying Vascular Calcification. Int J Mol Sci 2020;21:2204.
27. Vlachopoulos C, Aznaouridis K, Stefanadis C. Prediction of cardiovascular events and all-cause mortality with arterial stiffness: a systematic review and meta-analysis. J Am Coll Cardiol 2010;55:1318-1327.
28. Townsend RR, Wilkinson IB, Schiffrin EL, Avolio AP, Chirinos JA, Cockcroft JR, Heffernan KS, Lakatta EG, McEniery CM, Mitchell GF, Najjar SS, Nichols WW, Urbina EM, Weber T; American Heart Association Council on Hypertension. Recommendations for Improving and Standardizing Vascular Research on Arterial Stiffness: A Scientific Statement From the American Heart Association. Hypertension 2015;66:698-722.

29. Nilsson PM. Hemodynamic Aging as the Consequence of Structural Changes Associated with Early Vascular Aging (EVA). Aging Dis 2014;5:109-113.
30. Ben-Shlomo Y, Spears M, Boustred C, May M, Anderson SG, Benjamin EJ, Boutouyrie P, Cameron J, Chen CH, Cruickshank JK, Hwang SJ, Lakatta EG, Laurent S, Maldonado J, Mitchell GF, Najjar SS, Newman AB, Ohishi M, Pannier B, Pereira T, Vasan RS, Shokawa T, Sutton-Tyrell K, Verbeke F, Wang KL, Webb DJ, Willum Hansen T, Zoungas S, McEniery CM, Cockcroft JR, Wilkinson IB. Aortic pulse wave velocity improves cardiovascular event prediction: an individual participant meta-analysis of prospective observational data from 17,635 subjects. J Am Coll Cardiol 2014;63:636-646.
31. Dao HH, Essalihi R, Bouvet C, Moreau P. Evolution and modulation of age-related medial elastocalcinosis: impact on large artery stiffness and isolated systolic hypertension. Cardiovasc Res 2005;66:307-317.
32. Cavalcante JL, Lima JA, Redheuil A, Al-Mallah MH. Aortic stiffness: current understanding and future directions. J Am Coll Cardiol 2011;57:1511-1522.
33. Joly L, Mandry D, Verger A, Labat C, Watfa G, Roux V, Karcher G, Marie PY, Benetos A. Influence of Thoracic Aortic Inflammation and Calcifications on Arterial Stiffness and Cardiac Function in Older Subjects. J Nutr Health Aging 2016;20:347-354.

34. Guo J, Fujiyoshi A, Willcox B, Choo J, Vishnu A, Hisamatsu T, Ahuja V, Takashima N, Barinas-Mitchell E, Kadota A, Evans RW, Miura K, Edmundowicz D, Masaki K, Shin C, Kuller LH, Ueshima H, Sekikawa A; ERA JUMP Study Group. Increased Aortic Calcification Is Associated With Arterial Stiffness Progression in Multiethnic Middle-Aged Men. Hypertension 2017;69:102-108.

Table 1 Sources and dilution of the antibodies

Antibody	Catalog	Source	Dilution
pPERK	3179	Cell Signaling Technology	1: 500
PERK	ab65142	Abcam	1: 1000
peIF2α	9721	Cell Signaling Technology	1: 500
eIF2	9722	Cell Signaling Technology	1: 1000
ATF4	ab23760	Abcam	1: 2000
CHOP	ab10444	Abcam	1: 500
pIRE1	ab48187	Abcam	1: 2000
IRE1	ab37073	Abcam	1: 1000
XBP1	ab37152	Abcam	1: 500
ATF6	ab203119	Abcam	1: 500
calponin	ab203047	Abcam	1: 1000
SM22α	ab14106	Abcam	1: 2000
RUNX2	ab114133	Abcam	1: 1000
BMP2	ab14933	Abcam	1: 1000
β-actin	GTX109639	GeneTex	1: 2000
Second antibody	GTX213110	GeneTex	1: 5000~10000

Legends of Figures

Fig. 1. ISRIB treatment ameliorated VC induced by VDN in rats. A Alizarin red staining of the aorta; **B** and **C** Calcium content and ALP activity in the aorta. **P* < 0.05 vs. control group; #*P* < 0.05 vs. ISRIB group; !*P* < 0.05 vs. VC group. *n* = 8 in each group.

Fig. 2. ISRIB treatment ameliorated aortic stiffness induced by VC. A Systolic blood pressure (SBP); **B** pulse pressure (PP); **C** pulse wave velocity (PWV). **P* < 0.05 vs. control group; #*P* < 0.05 vs. ISRIB group; !*P* < 0.05 vs. VC group. *n* = 8 in each group.

Fig. 3. ISRIB treatment ameliorated trans-differentiation of VSMCs from a contractile to an osteoblastic type. **A** Representative images of Western blots; **B**–**E** Quantitative analysis of the protein levels of calponin, SM22 α , RUNX2, and BMP2. **P* < 0.05 vs. control group; #*P* < 0.05 vs. ISRIB group; !P < 0.05 vs. VC group. *n* = 8 in each group.

Fig. 4. ISRIB treatment ameliorated stimulation of ERS in the calcified aorta. **A** Representative images of Western blots; **B**–**D** Quantitative analysis of the protein levels of GRP94, GRP78, and CHOP. **P* < 0.05 vs. control group; #*P* < 0.05 vs. ISRIB group; !*P* < 0.05 vs. VC group. *n* = 8 in each group.

Fig. 5. ISRIB treatment ameliorated stimulation of eIF2/ATF4 signaling in calcified aorta. **A** Representative images of Western blots; **B**–**D** Quantitative analysis of the protein levels for pPERK, peIF2, and ATF4. **P* < 0.05 vs. control group; $^{\#}P$ < 0.05 vs. ISRIB group; $^{!}P$ < 0.05 vs. VC group. *n* = 8 in each group.

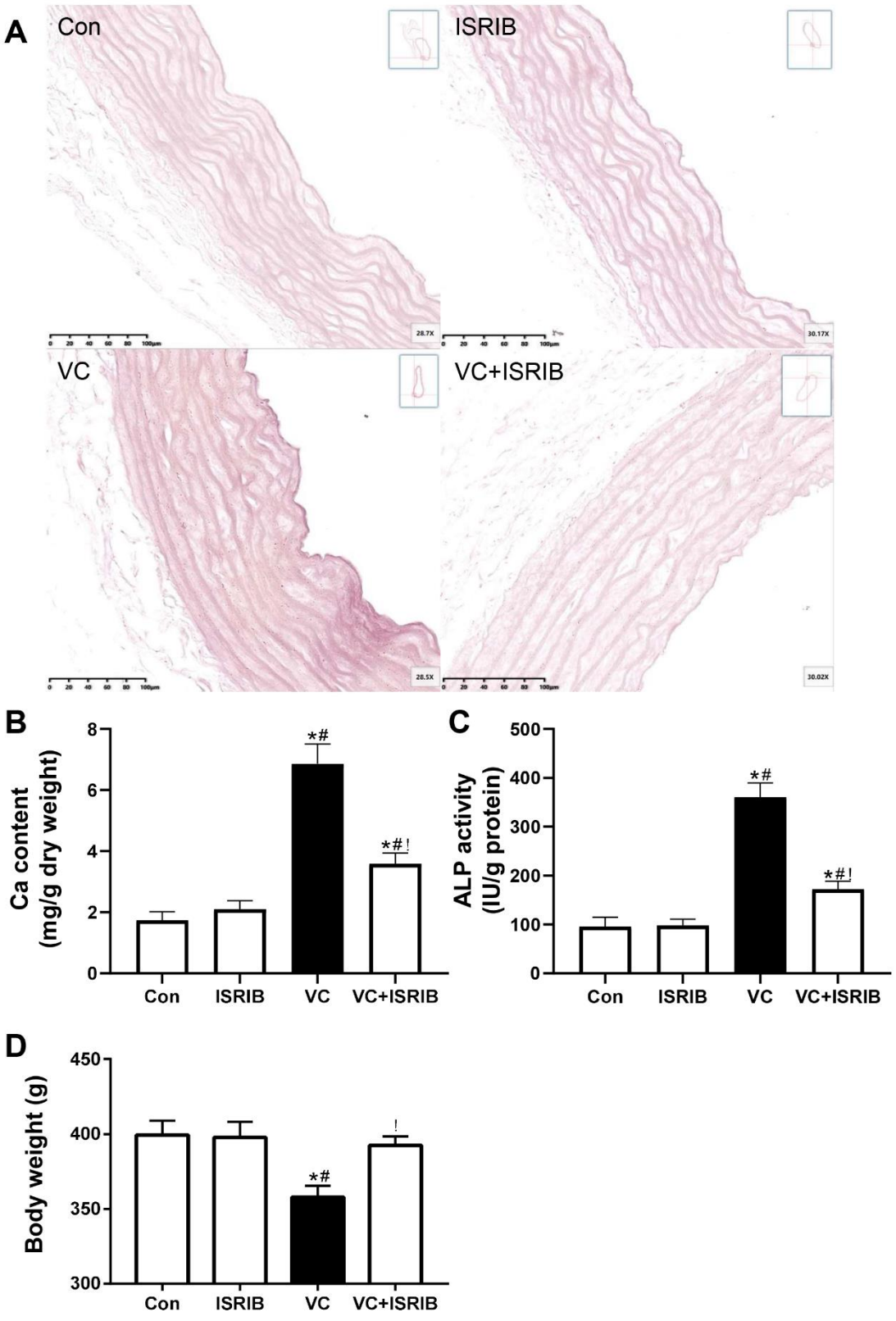
A
Con
ISRIB
VC
VC+ISRIB
B
Ca content (mg/g dry weight)
0
2
4
6
8
*#
*#!
Con
ISRIB
VC
VC+ISRIB
C
ALP activity (IU/g protein)
0
100
200
300
400
500
*#
*#!
Con
ISRIB
VC
VC+ISRIB
D
Body weight (g)
300
350
400
450
*#
!
Con
ISRIB
VC
VC+ISRIB

Fig 1

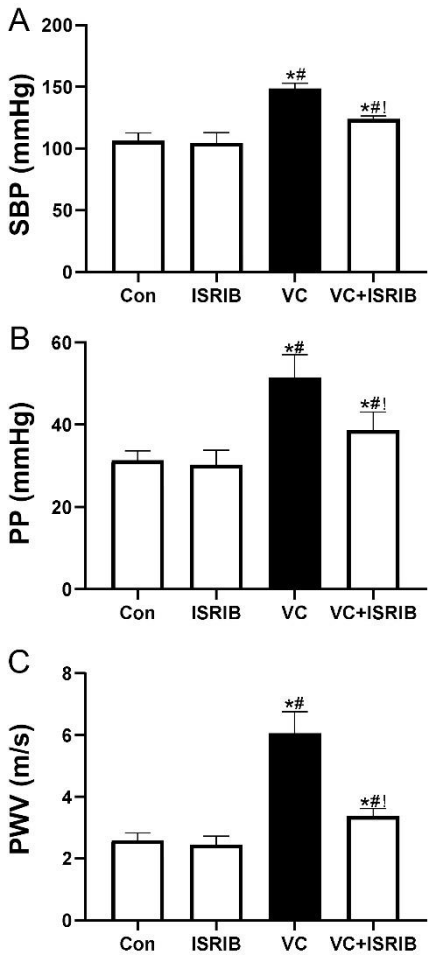
A
SBP (mmHg)
200
150
100
50
0
*#
*#!
Con
ISRIB
VC
VC+ISRIB
B
PP (mmHg)
60
40
20
0
*#
*#!
Con
ISRIB
VC
VC+ISRIB
C
PWV (m/s)
8
6
4
2
0
*#
*#!
Con
ISRIB
VC
VC+ISRIB

Figure 2

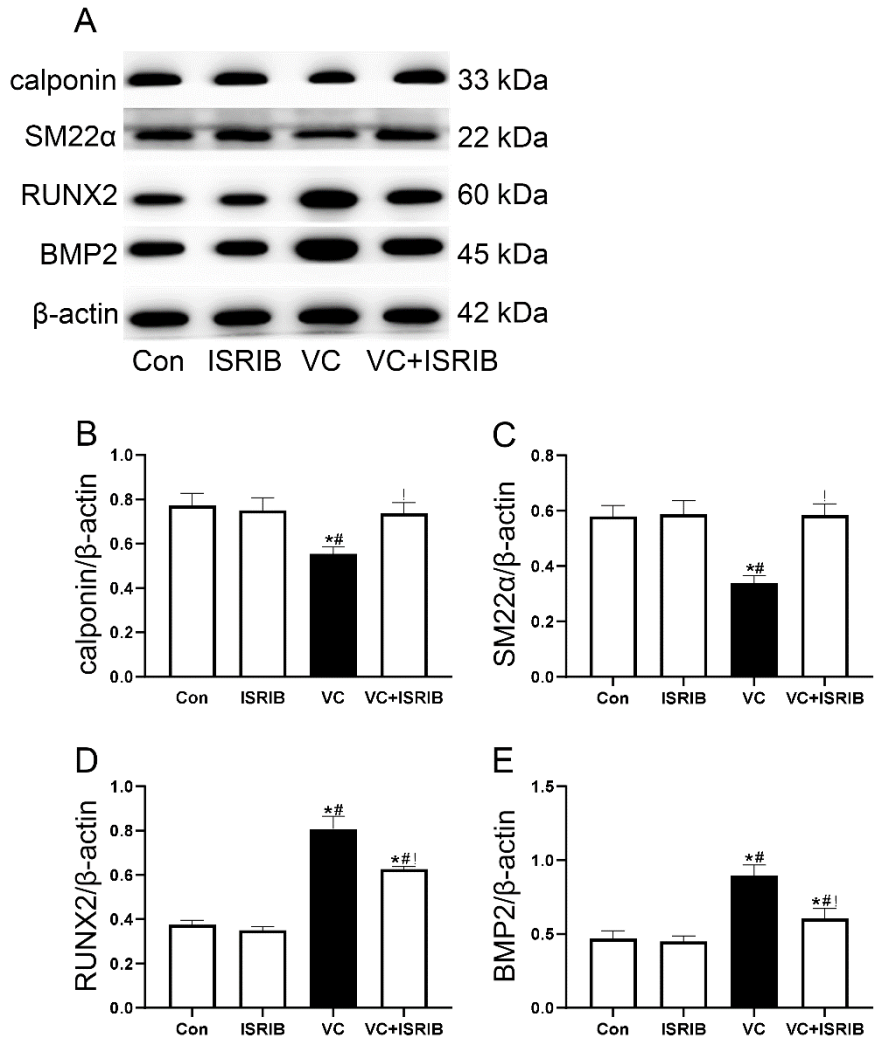
A
calponin
SM22α
RUNX2
BMP2
β-actin
33 kDa
22 kDa
60 kDa
45 kDa
42 kDa
Con ISRIB VC VC+ISRIB
B
calponin/β-actin
C
SM22α/β-actin
D
RUNX2/β-actin
E
BMP2/β-actin
Con
ISRIB
VC
VC+ISRIB
*#
*#!

Figure 3

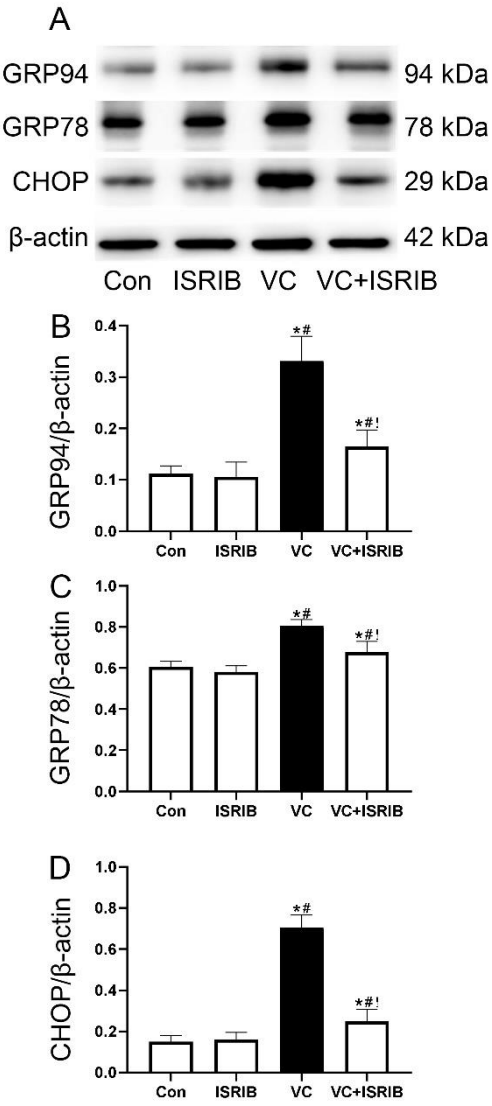
A
GRP94
GRP78
CHOP
β-actin
94 kDa
78 kDa
29 kDa
42 kDa
Con ISRIB VC VC+ISRIB
B
GRP94/β-actin
C
GRP78/β-actin
D
CHOP/β-actin
*#
*#!
Con
ISRIB
VC
VC+ISRIB

Figure 4

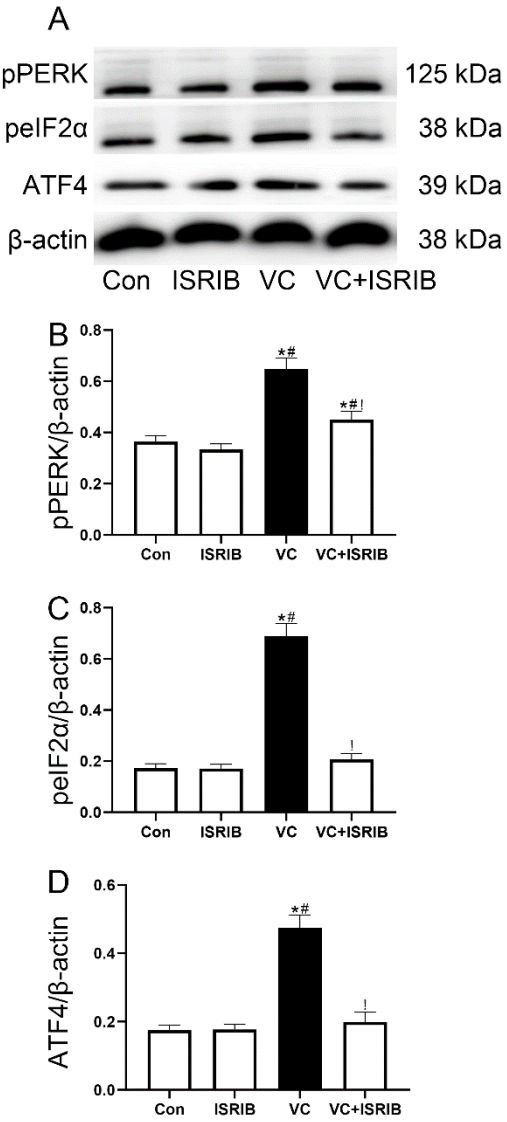
A
pPERK
peIF2α
ATF4
β-actin
125 kDa
38 kDa
39 kDa
38 kDa
Con ISRIB VC VC+ISRIB
B
pPERK/β-actin
C
peIF2α/β-actin
D
ATF4/β-actin
0.0
0.2
0.4
0.6
0.8
*#
*#!
!
Con
ISRIB
VC
VC+ISRIB

Figure 5